Electronic Supplementary Material (ESI) for Journal of Materials Chemistry C.

Polymorphic Crystals and Their Luminescence Switching of Triphenylacrylonitrile Derivatives upon Solvent Vapor, Mechanical, and Thermal Stimuli

Yujian Zhang,[ab] Qingbao Song,[a] Kai Wang,[d] Wengang Mao,[a] Feng Cao,[b] Jingwei Sun,[a] Lingling Zhan,[a] Yaokang Lv,[a] Yuguang Ma,[c] Bo Zou,*[d] and Cheng Zhang*[a]

[a]Country College of Chemical Engineering, Zhejiang University of Technology, Caowang Road No.18, Hangzhou, P. R. China
E-mail: czhang@zjut.edu.cn

[b]Department of Materials chemistry, Huzhou university, Xueshi Road No.1, Huzhou, P. R. China

[c]State Key Laboratory of Luminescent Materials and Devices, South China University of Technology, Guangzhou, P. R. China

[d]State Key Laboratory of superhard materials, Jilin University, 2699 Qianjin Avenue, Changchun, P. R. China
E-mail: zoubo@jlu.edu.cn

Experimental Section

Instrumentation

Nuclear magnetic resonance (NMR) spectra in solution were recorded on a Bruker Avance III 500-MHz spectrometer at 298 K using chloroform-d ($CDCl_3$) as solvent and tetramethylsilane as standard. The splitting patterns are designated as follows: s (singlet); d (doublet); t (triplet); m (multiplet). Mass spectroscopy was recorded with a Thermo LCQ Fleet MS spectrometer. The UV-vis spectrum and steady-state Fluorescent measurements was recorded on a Uv-2600 Uv-vis spectrophotometer (Shimadzu, Japan) and Perkine Elmer LS-55 spectro-photometer, respectively. Digital photographs were taken by 550D (Canon, Japan) digital cameras. The Φ_f of crystal was determined by using a calibrated integrating sphere system (errors 5%). Powder XRD measurements were conducted on X'Pert PRO diffractometer (CuKα) in the range $5 < 2\theta < 40$ (PANalytical, Netherlands). X-ray crystallographic intensity data were collected using a Xcalibur, Eos, Gemini Ultra CCD diffractometer equipped with a graphite monochromated Enhance (Mo) X-ray source (λ = 0.71073 Å). Fluorescence lifetimes were measured by a FLS920 time-corrected single photon counting system (Edinburgh, England). The situ steady-state PL measurements at the low temperature are tested on Fluorolog-3-TAU (Horiba JY, France). High-pressure experiments: The tiny crystal was placed in the hole (diameter: 200 mm) of a T301 steel gasket, A 4:1 mixture of methanol and ethanol was used as a pressure transmitting medium (PTM). The situ steady-state PL measurements under high pressure were performed on a QuantaMaster 40 spectrometer (produced by Photon Technology Inc.) in the reflection mode. The 405 nm line of a violet diode laser with a spot size of 20 mm and a power of 100 mW was used as the excitation source. The diamond anvil cell (DAC) containing the sample was put on a Nikon fluorescence microscope to focus the laser on the sample. Optical photographs of the compressed TPAN-MeO samples were obtained using an imaging camera (Canon EOS 5D Mark II) equipped on the fluorescence microscope.

Materials

THF and other solvents were distillated and dried prior to utilization. All other starting materials were purchased from **Alfa** and **Aldrich**, and used as received.

Synthesis and structural characterization of TPAN-MeO

The synthetic routes to the triphenylacrylonitrile derivative **TPAN-MeO** are depicted in Scheme S1. The intermediate TPCN-Br was prepared according to previous procedures.[8]

And then, the Suzuki coupling reaction of 4-methoxyphenylboronic acid with **TPAN-Br** catalyzed by $Pd(PPh_3)_4$, for 32 h at 90 ℃, gave desired product TPCN-OMe in 65.7% yield. ^1H NMR (500 MHz, $CDCl_3$) δ 7.53 (d, J = 8.5 Hz, 2H), 7.51 - 7.47 (m, 2H), 7.48 - 7.42 (m, 5H), 7.34 (d, J = 8.5 Hz, 2H), 7.30 (t, J = 7.5 Hz, 1H), 7.24 (t, J = 7.5 Hz, 2H), 7.09 (d, J = 7.0 Hz, 2H), 6.99 (d, J = 9.0 Hz, 2H), 3.87 (s, 3H). ^{13}C NMR (125 MHz, $CDCl_3$) δ 159.47, 157.33, 140.54, 140.52, 139.20, 133.02, 132.45, 130.75, 130.08, 129.94, 129.83, 128.99, 128.43, 128.32, 127.99, 126.46, 120.12, 114.26, 111.35, 129.94, 129.83, 128.99, 128.43, 128.32, 127.99, 126.46, 120.12, 114.26, 111.35, 55.33. MS(EI) m/e 387.5 [M^+].

Crystallographic data for **BCrys**: $C_{28}\,H_{21}N_1O_1$, M = 387.46 g/mol, monoclinic, a = 11.0759(7) Å, b = 29.6119(13) Å, c= 7.7409(4) Å; α= 90 °, β = 122.900(5) °, γ= 90 °, V = 2131.7(2) Å^3, T = 153 K, space group: Cc, D_{calc} = 1.207 g/cm^3, S= 1.024, R(int)= 0.0224, Z = 4, The final R indices were R_1 = 0.0379(2162),ωR_2 = 0.0771(2811) [$I > 2\sigma(I)$], CCDC= 1032464

Crystallographic data for **SCrys**: $C_{28}\,H_{21}N_1O_1$, M = 387.46 g/mol, Triclinic, a = 10.0340(3) Å, b = 10.1300(3) Å, c= 23.5530(6) Å; α= 77.824(2) °, β = 84.358(2) °, γ= 65.810(3) °, V = 2131.7(2) Å^3, T = 293(2) K, space group: P-1, D_{calc} = 1.206 g/cm^3, S= 1.024, R(int)= 0.0349, Z = 4, The final R indices were R_1 = 0.0482(6501), ωR_2 = 0.0771(2811) [$I > 2\sigma(I)$], CCDC= 1032465

Crystallographic data for **YCrys**: $C_{28}\,H_{21}N_1O_1$, M = 387.46 g/mol, *Monoclinic*, a = 9.96960(1) Å, b = 43.1553(3) Å, c= 10.08110(1) Å; α= 90 °, β = 98.7640(1) °, γ= 90 °, V = 4286.66(7) Å^3, T = 293(2) K, space group: P2(1)/n, D_{calc} = 1.201 g/cm^3, S= 0.999, R(int)= 0.0189, Z = 8, The final R indices were R_1 = 0.0432(7455), ωR_2 = 0.1322(8025) [$I > 2\sigma(I)$], CCDC= 1032466

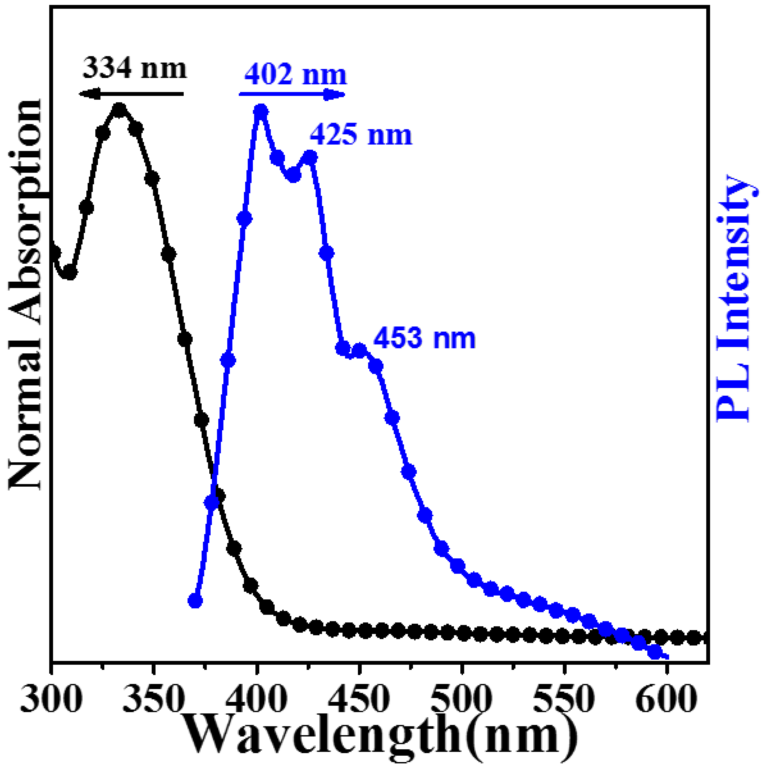

Figure S1 the absorption spectra and PL spectra of luminogens **TPAN-MeO** in THF (10 μm)

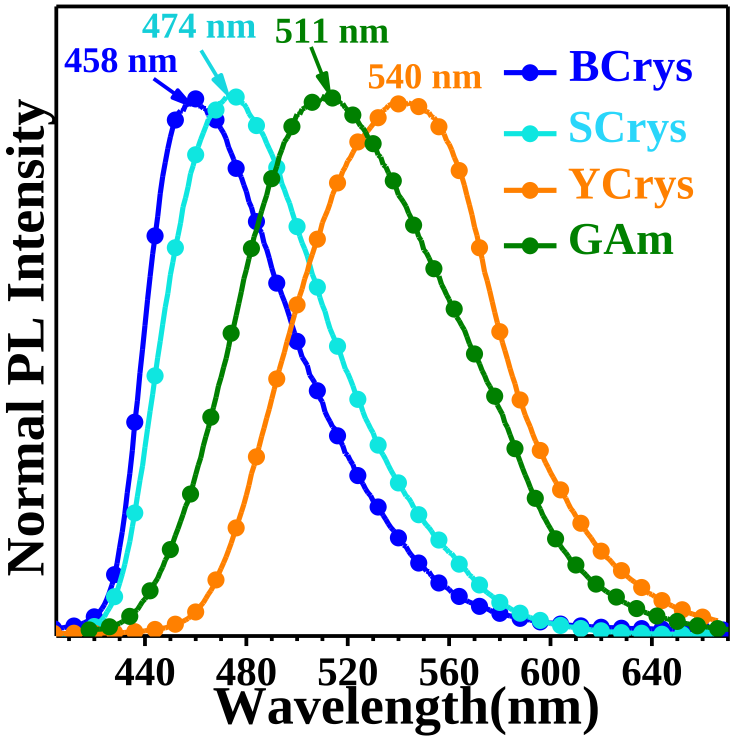

Figure S2 PL spectra of luminogens TPAN-MeO in the different aggregated states (BCrys, SCrys, YCrys and GAm)

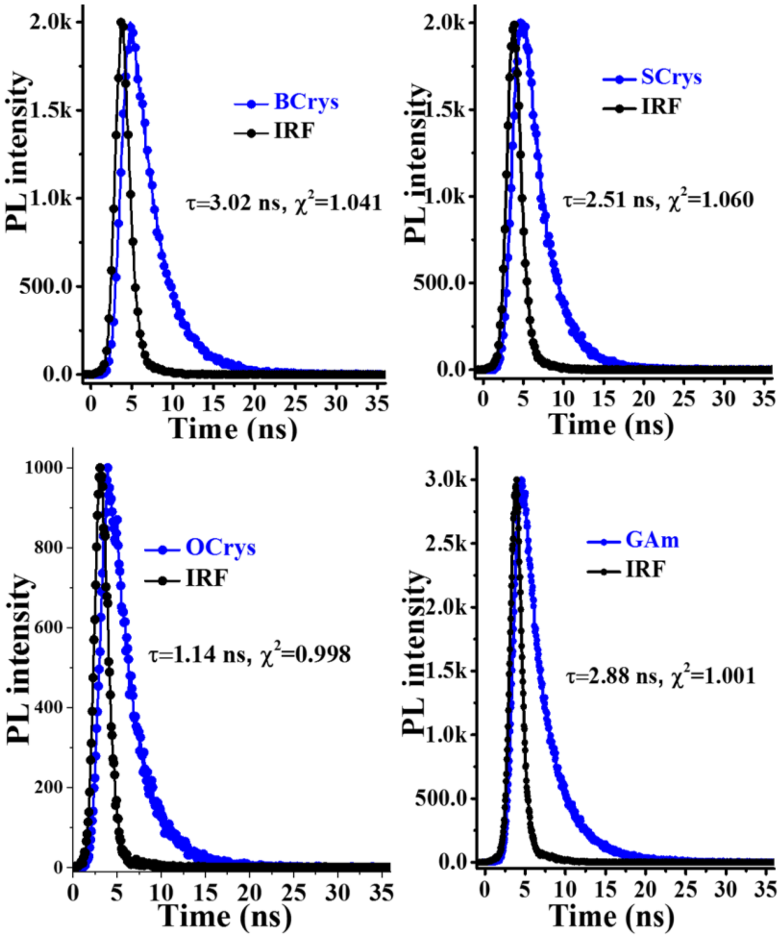

Figure S3 Transient state fluorescence spectra (fluorescence lifetime) of luminogens **TPAN-MeO** in the different aggregated states (BCrys, SCrys, YCrys and GAm)

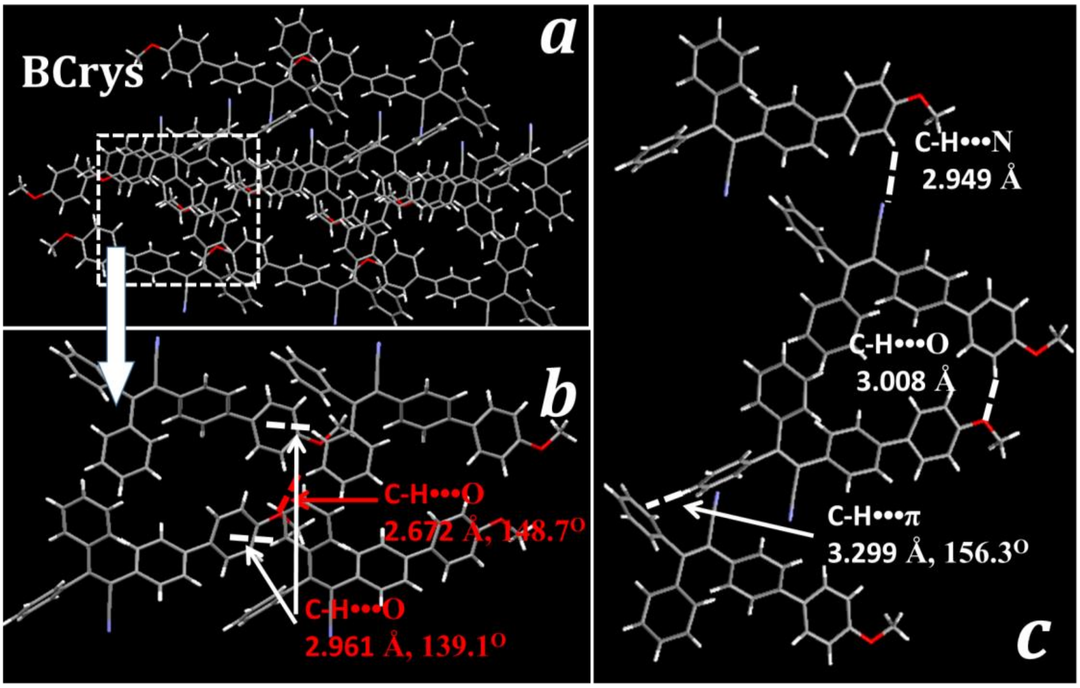

Figure S4 Molecular stacking structure with secondary bonding interactions(C-H•••π, C-H•••O) in the crystal **BCrys.**

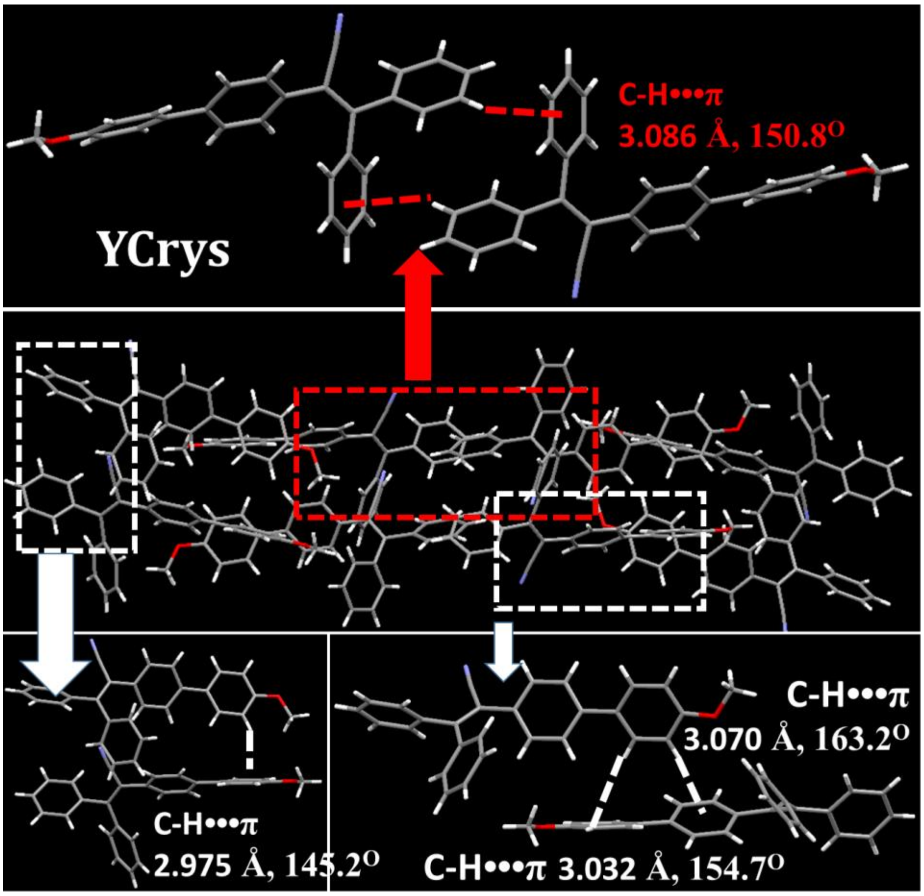

Figure S5 Molecular stacking structure with secondary bonding interactions(C-H•••π) in the crystal **YCrys.**

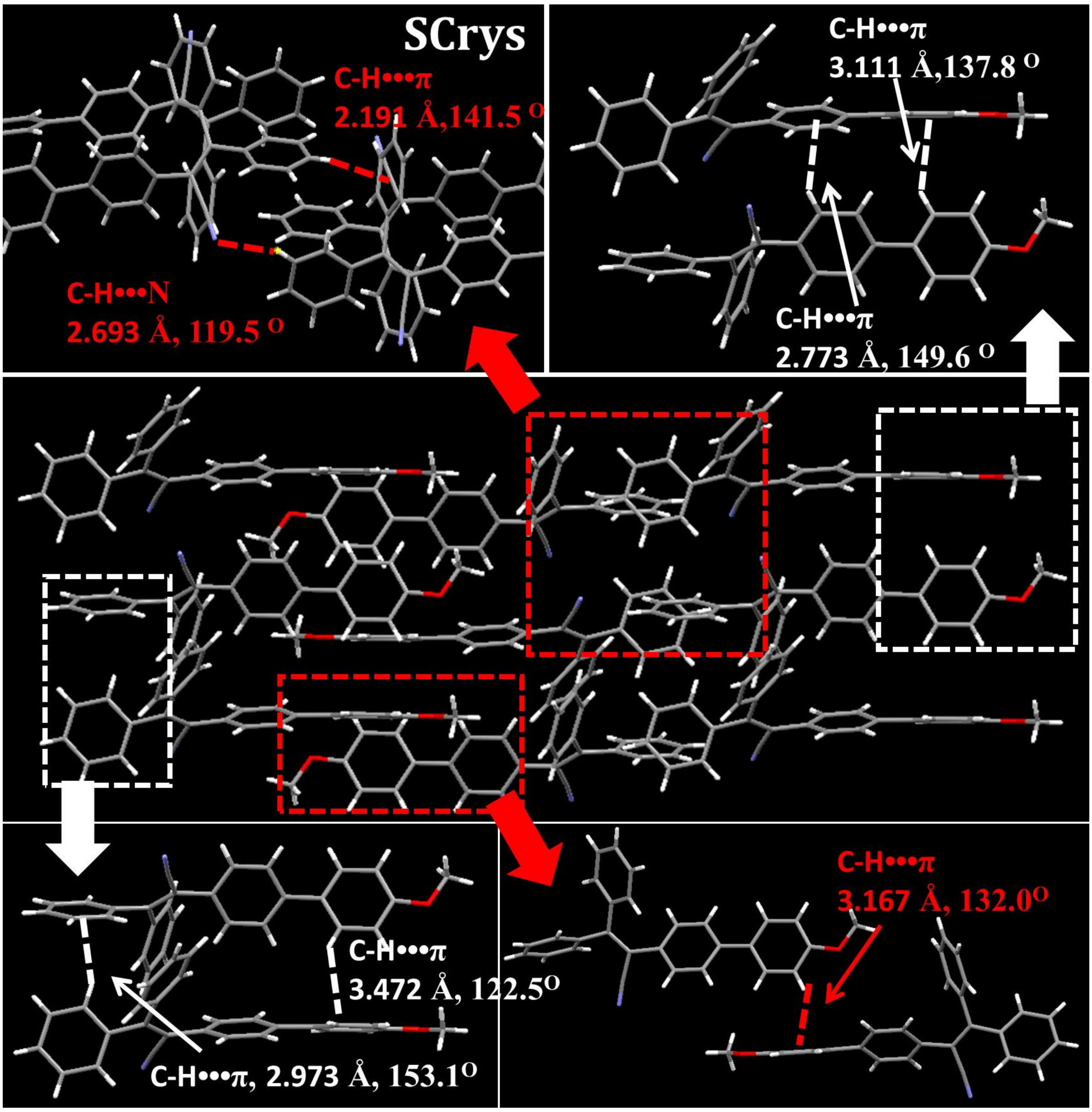

Figure S6 Molecular stacking structure with secondary bonding interactions(C-H•••π, C-H•••N) in the crystal **SCrys.**

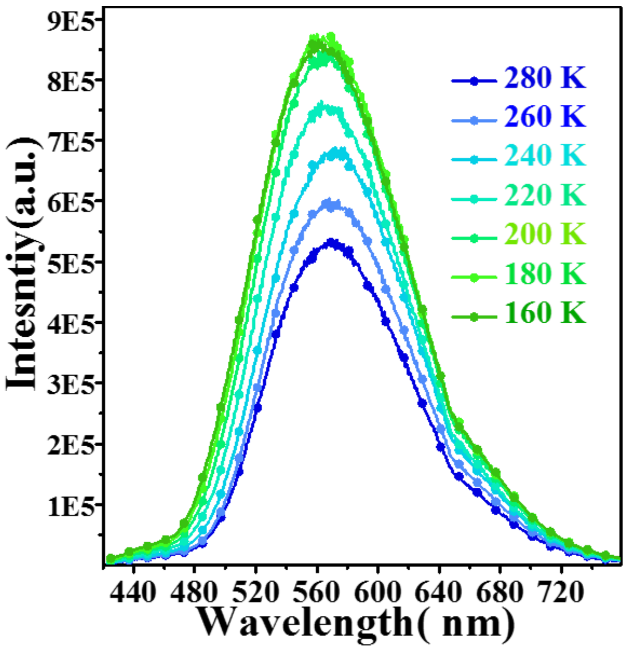

Figure S7 PL spectra of crystal YCrys at the different temperature (280k-160k)

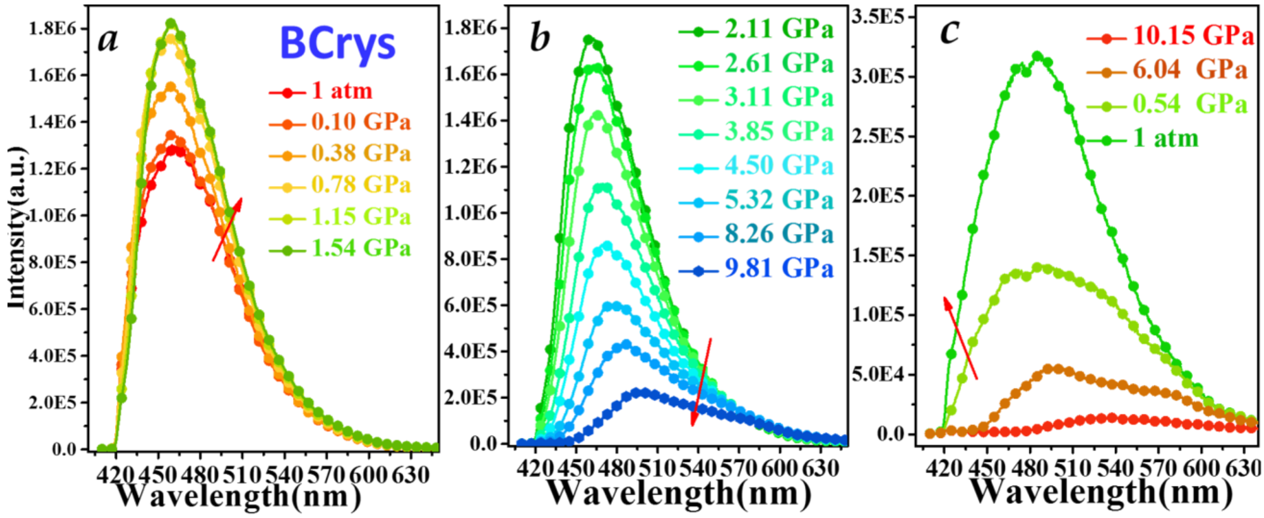

Figure S8 Fluorescence spectra of crystal BCrys under the hydrostatic pressure from compression (a, b) to decompression (c).

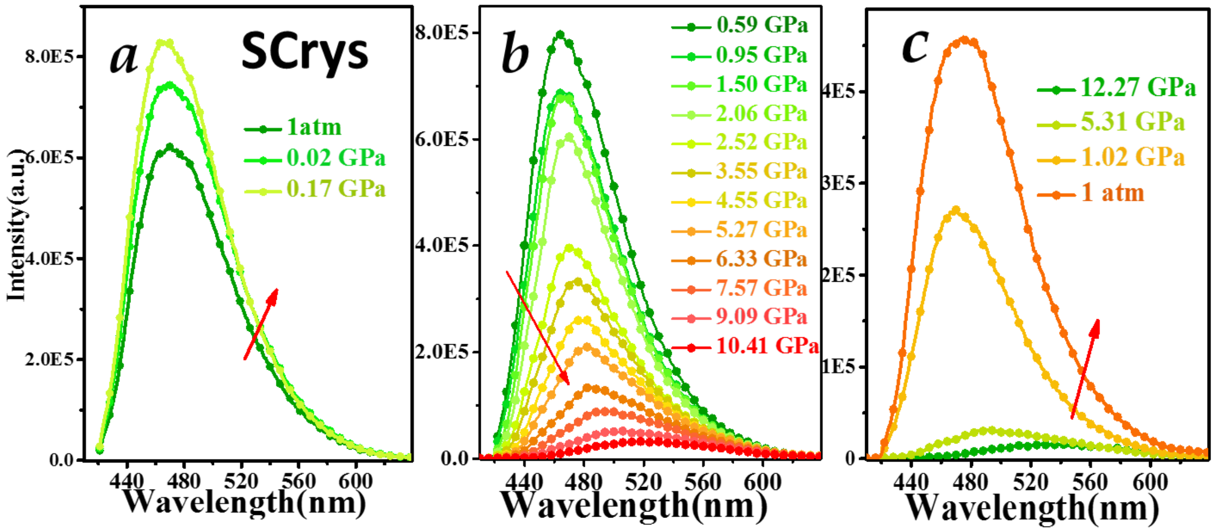

Figure S9 Fluorescence spectra of crystals SCrys under the hydrostatic pressure from compression (a, b) to decompression (c).

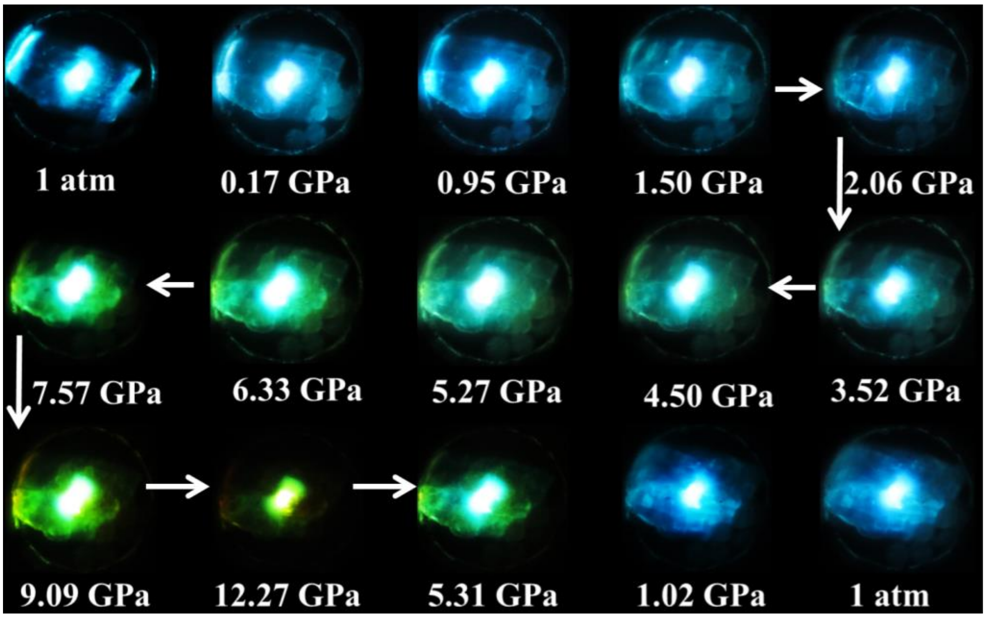

Figure S10 Fluorescence images of crystal **SCrys** under the hydrostatic pressure (from the compression to decompression)

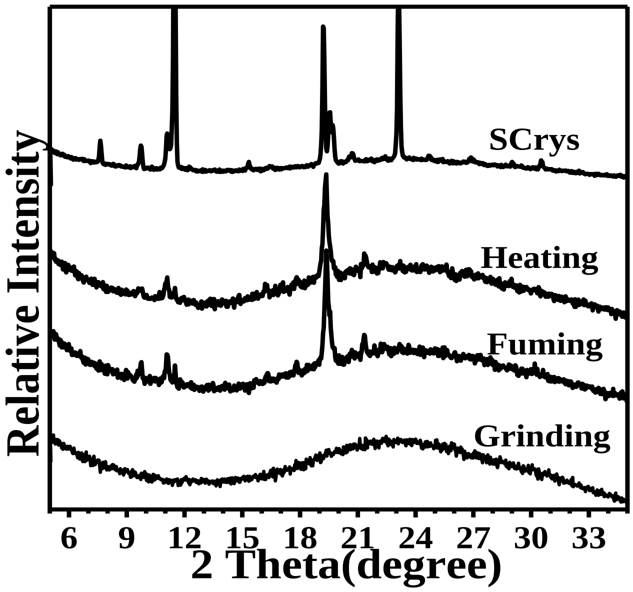

Figure S11 The powders XRD profiles of crystals SCrys at the different states; Heating treatments: after heating above 70 °C for 30 min; Fuming treatments: n-hexane vapor.

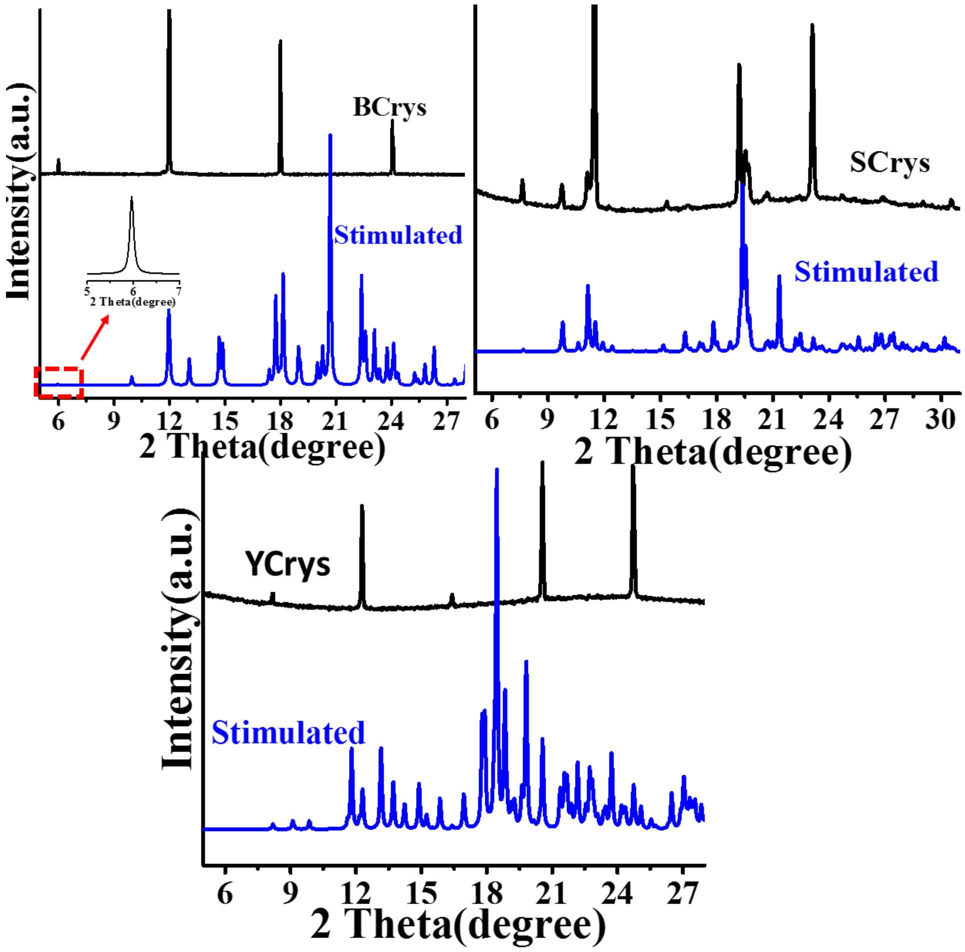

Figure S12 Powder XRD patterns of TPAN-MeO in different state (BCrys, SCrys, YCrys) and the simulated powder XRD pattern of single crystals

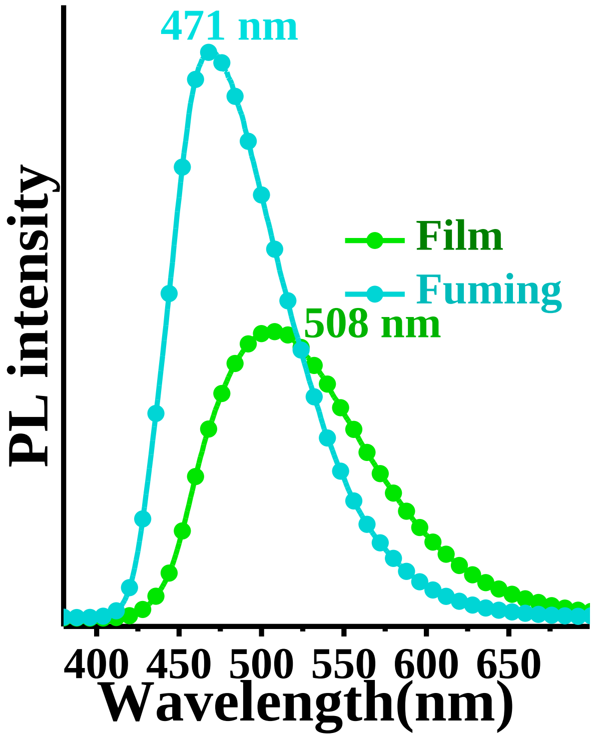

Figure S13 PL spectra of film prepared by the drop-casting and upon exposure to n-hexane vapor

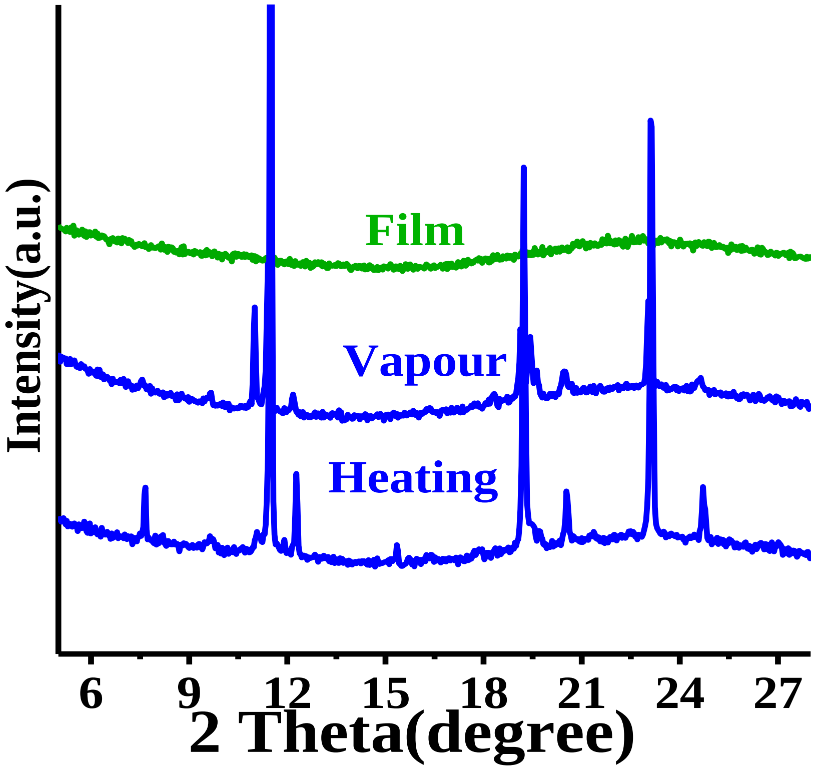

Figure S14 Powder XRD patterns of TPAN-MeO film in the different state (upon multi-stimuli.)